Acta Pharmacologica Sinica

www.nature.com/aps

ARTICLE

# Metrnl regulates cognitive dysfunction and hippocampal BDNF levels in D-galactose-induced aging mice

Chen Hong[1,2], Zhi Wang[1], Si-li Zheng[1], Wen-jun Hu[1], Shu-na Wang[1], Yan Zhao[1] and Chao-yu Miao[1]

Aging is one of the main risk factors for cognitive dysfunction. During aging process, the decrease of brain-derived neurotrophic factor (BDNF) and the impairment of astrocyte function contribute to the cognitive impairment. Metrnl, a neurotrophic factor, promotes neural growth, migration and survival, and supports neural function. In this study, we investigated the role of Metrnl in cognitive functions. D-galactose (D-gal)-induced aging model was used to simulate the process of aging. Cognitive impairment was assessed by the Morris water maze test. We showed that Metrnl expression levels were significantly increased in the hippocampus of D-gal-induced aging mice. Metrnl knockout did not affect the cognitive functions in the baseline state, but aggravated the cognitive impairment in the D-gal-induced aging mice. Furthermore, Metrnl knockout significantly reduced hippocampal BDNF, TrkB, and glial fibrillary acidic protein (GFAP) levels in the D-gal-induced aging mice. In the D-gal-induced aging cell model in vitro, Metrnl levels in the hippocampal astrocytes were significantly increased, and Metrnl knockdown and overexpression regulated the BDNF levels in primary hippocampal astrocytes rather than in neurons. We conclude that Metrnl regulates cognitive functions and hippocampal BDNF levels during aging process. As a neurotrophic factor and an endogenous protein, Metrnl is expected to become a new candidate for the treatment or alleviation of aging-related cognitive dysfunction.

**Keywords:** Metrnl; aging; cognitive impairment; BDNF; hippocampus; astrocytes

*Acta Pharmacologica Sinica* (2023) 44:741–751; https://doi.org/10.1038/s41401-022-01009-y

## INTRODUCTION

Learning and memory are important cognitive functions [1]. In humans, impaired learning and memory functions are typical features of dementia, which seriously affects the quality of life, and might even lead to death [2, 3]. Aging is the most prevalent cause of dementia, and the situation is worsening due to the rapid increase in the elderly population [2–4]. However, the etiology and pathogenesis of aging-related dementia are still unclear, the drugs for improving cognitive functions are limited and the treatment of dementia is inadequate [5, 6].

Metrnl is a secreted protein that was identified by our laboratory as a novel adipokine (also known as Subfatin) [7]. Metrnl is abundant in subcutaneous white adipose tissue and barrier tissues, including the skin and the intestinal and respiratory tract epithelium. It regulates insulin sensitivity, lipid metabolism, inflammatory response, and intestinal functions [8–13]. Two studies have investigated the role of Metrnl in the central nervous system (CNS). One study reported that there were four genes, including *METRNL*, lost in the chromosome 17 of humans with mild ring 17 syndrome (a rare disorder with clinical features of mental retardation, growth delay, seizures, etc.) [14]. The other study reported that Metrnl was a neurotrophic factor that can promote neurite outgrowth and subventricular zone neuroblast migration in vitro and support the survival and function of spiral ganglion neurons in deafened guinea pigs [15]. These studies suggested that Metrnl is a neurotropic factor that might be related to cognitive functions.

D-galactose (D-gal) is an aldohexose that exists in the normal metabolic process. However, a long-term overdose of D-gal causes systemic oxidative stress, inflammation, apoptosis, a decrease in brain-derived neurotrophic factor (BDNF) levels, and cognitive dysfunction, which mimics aging to a certain degree [16]. The D-gal-induced aging model is widely used for pharmacodynamic evaluation and studying the mechanism of aging and aging-related cognitive impairment [17, 18].

The role of Metrnl in the CNS is not fully elucidated, and the function of Metrnl in the cognitive functions, especially in aging-related cognitive impairment also has not been reported. Therefore, in this study, we used D-gal-induced aging model to simulate aging and determined the role of Metrnl in aging-related cognitive dysfunction. Our study might elucidate the efficacy of Metrnl in the treatment of cognitive impairment.

## MATERIALS AND METHODS

### Animals and the generation of Metrnl knockout mice

All animal experiments were performed following the National Institutes of Health Guide for the Care and Use of Laboratory Animals and approved by the Institutional Animal Care and Use Committee of the Second Military Medical University. All animals

[1]Department of Pharmacology, Second Military Medical University/Naval Medical University, Shanghai 200433, China and [2]Present address: State Key Laboratory of Trauma, Burns and Combined Injury, Shock and Transfusion Department, Research Institute of Surgery, Daping Hospital, Army Medical University, Chongqing 400042, China
Correspondence: Chao-yu Miao (cymiao@smmu.edu.cn)
These authors contributed equally: Chen Hong, Zhi Wang

Received: 1 April 2022 Accepted: 25 September 2022
Published online: 13 October 2022

**Table 1.** Primer sets used in the study.

| Gene | Forward primer (5′-3′) | Reversed primer (5′-3′) |
|---|---|---|
| GAPDH | GGGTCCCAGCTTAGGTTCAT | CCCAATACGGCCAAATCCGT |
| Metrnl | CTGGAGCAGGGAGGCTTATTT | GGACAACAAAGTCACTGGTACAG |
| TrkB | CTGGGGCTTATGCCTGCTG | AGGCTCAGTACACCAAATCCTA |
| BDNF | TCATACTTCGGTCATGAAGG | ACACCTGGGTAGGCCAAGTT |

were acclimated to the laboratory environment for one week and housed in a standard animal room with a 12 h/12 h dark/light cycle at 22–26 °C and 40%–70% humidity. Ella-Cre mice and C57BL/6 mice were purchased from the Shanghai Research Center for Model Organisms (Shanghai, China).

Metrnl floxed mice (Metrnl$^{loxP/loxP}$), Ella-Cre mice, and C57BL/6 mice were used to generate Metrnl knockout mice (Metrnl$^{-/-}$). The targeting construct of Metrnl$^{loxP/loxP}$ was characterized in our previous study [8]. Briefly, three loxP sequences were inserted into the Metrnl allele to flank exon 3 and the coding region of exon 4, which could be excised by Cre recombinase. Ella-Cre mice, which target the expression of Cre recombinase to the stages of mouse oocytes and preimplantation embryos, were used to generate Metrnl knockout mice [19]. To obtain Metrnl knockout mice, initially, Metrnl$^{loxP/loxP}$ mice were crossed with Ella-Cre mice to generate Metrnl$^{+/-}$Ella-Cre mice. These mice were crossed with C57BL/6 mice to generate Metrnl$^{+/-}$ mice. Finally, Metrnl$^{+/-}$ mice were inbred to generate Metrnl$^{-/-}$ mice [11].

### Preparation of D-gal-induced aging mouse model

Metrnl knockout mice and wild-type control mice were used to prepare the D-gal-induced aging model according to the standard procedure [17]. Briefly, the mice were intraperitoneally injected with D-gal (100 mg·kg$^{-1}$·d$^{-1}$; Sangon Biotech; China) for 60 days to establish the D-gal-induced aging mouse model. The control group was intraperitoneally injected with an equal volume of saline as vehicle control.

### Morris water maze test

The experimental device was located in a separate laboratory to avoid external interference. We performed the test in a black circular pool (120 cm in diameter and 45 cm in height) with visual cues of different colors and shapes of plastic plates hanging on the shelf. Four illuminants were presented outside the curtain to increase visibility. The pool was filled with opaque water using a nontoxic, water-soluble white dye and the temperature was kept at 22 ± 1 °C. It was divided into four quadrants. An invisible platform (10 cm in diameter) was placed in the center of one of the four quadrants and submerged 1 cm below the water surface. The behavior of the mice and their swimming paths were monitored by a video tracking system. The protocols were based on the reports of Vorhees and Williams [20]. Briefly, we conducted the test over six consecutive days. The spatial acquisition test was performed from days 1 to 5, and the probe trial was conducted on day 6. On the days of the spatial acquisition test, the mice were placed in four fixed positions in water but in a different order each day. In each trial, we let the mouse swim for 60 s in the pool to find the hidden platform. If it could not find the platform within 60 s, we guided it to the platform for 20 s. On day 6, we removed the platform and placed the mouse on the opposite quadrant of the platform for 60 s. Escape latency and total distance were monitored during the spatial acquisition test to analyze the learning ability. The frequency of crossing the platform and the time spent in the target quadrant were monitored to analyze the memory function in the probe trial on day 6. The swimming speed was monitored to analyze the motor function. The average values of these parameters for each session and each mouse were evaluated.

### Primary hippocampal neuron and astrocyte culture

The protocols were based on published methods [21, 22]. Primary hippocampal neurons and astrocytes were cultured using similar steps but in different culture media. Hippocampal tissues were dissected from the cortex of newborn C57BL/6 mouse brains under the microscope. Then, the tissues were digested by StemPro® Accutase® Cell Dissociation Reagent (Life Technologies; Carlsbad, CA, USA) for 5–10 min at 37 °C in a constant temperature shaker. Suspensions of hippocampal neurons were planted for 4–6 h on poly-*D*-lysine-coated (Sigma–Aldrich; St. Louis, MO, USA) six wells (Corning; Midland, MI, USA) with DMEM containing 20% FBS. Then, the medium was replaced by Neurobasal®-A medium (Life Technologies; Carlsbad, CA, USA) mixed with 2% B27 (Life Technologies; Carlsbad, CA, USA), 25 μM GlutaMAX™-I Supplement (Life Technologies; Carlsbad, CA, USA) and 1% Penicillin-Streptomycin (Life Technologies; Carlsbad, CA, USA). To inhibit glial growth, 10 μM cytosine arabinoside (Sigma–Aldrich; St. Louis, MO, USA) was added the day after the neurons were planted. After being cultured for seven days, the mature neurons were stained by Tuj-1 (neuron marker; Millipore; Billerica, MA, USA) and glial fibrillary acidic protein (GFAP, astrocyte marker; Millipore; Billerica, MA, USA) to ensure that the proportion was higher than 90%. As for hippocampal astrocytes, the suspensions containing hippocampal astrocytes were planted in Petri dishes (6 cm in diameter) in DMEM containing 10% FBS. After 5–7 days of culture, the astrocytes were transferred to new plates and generally used in passage 1. All cells were cultured in the humidified incubator at 37 °C with 5% $CO_2$. Half of the medium was changed every two days.

### Preparation of D-gal-induced aging cell model

The D-gal-induced aging cell model was based on a previously described experimental method [23]. Briefly, primary hippocampal neurons and astrocytes were planted in the six-well plates and cultured for seven days following the above-mentioned method. On day 8, we changed the medium, added D-gal into the medium (the final concentration of D-gal was 10 mg/mL), cultured the cells for another 48 h, and used them to conduct further tests after changing the medium.

### Lentivirus-mediated overexpression and knockdown of Metrnl in neurocytes

The sequence 5′-CACGCTTTAGTGACTTTCAAA-3′ was used to construct the Metrnl shRNA lentivirus based on our previous study [8]. Human (Gene ID: 284207) and mouse Metrnl sequences (Gene ID: 210029) were used to construct Metrnl-expressing lentivirus [8]. The cells were infected with multiplicity of infection in a value of 20~30.

### Real-time PCR and Western blot

Real-time PCR and Western blot analyses were performed based on the methods described in our previous study [7]. To perform real-time PCR, the RNA was extracted with TRIzol (Invitrogen). The primers are listed in Table 1. To perform Western blot analysis, the antibodies used included the TrkB antibody (Cell Signaling #4603), the BDNF antibody (Abcam ab108319/ab205067), the Synaptophysin antibody (Abcam ab14692), the GFAP antibody (Abcam ab7260), the CD130 antibody (Abcam ab202850), the IL-6 antibody (Abcam ab7737), the STAT3 antibody (Santa Cruz sc-8019), the p-STAT3 antibody (Santa Cruz sc-8059), the Donkey

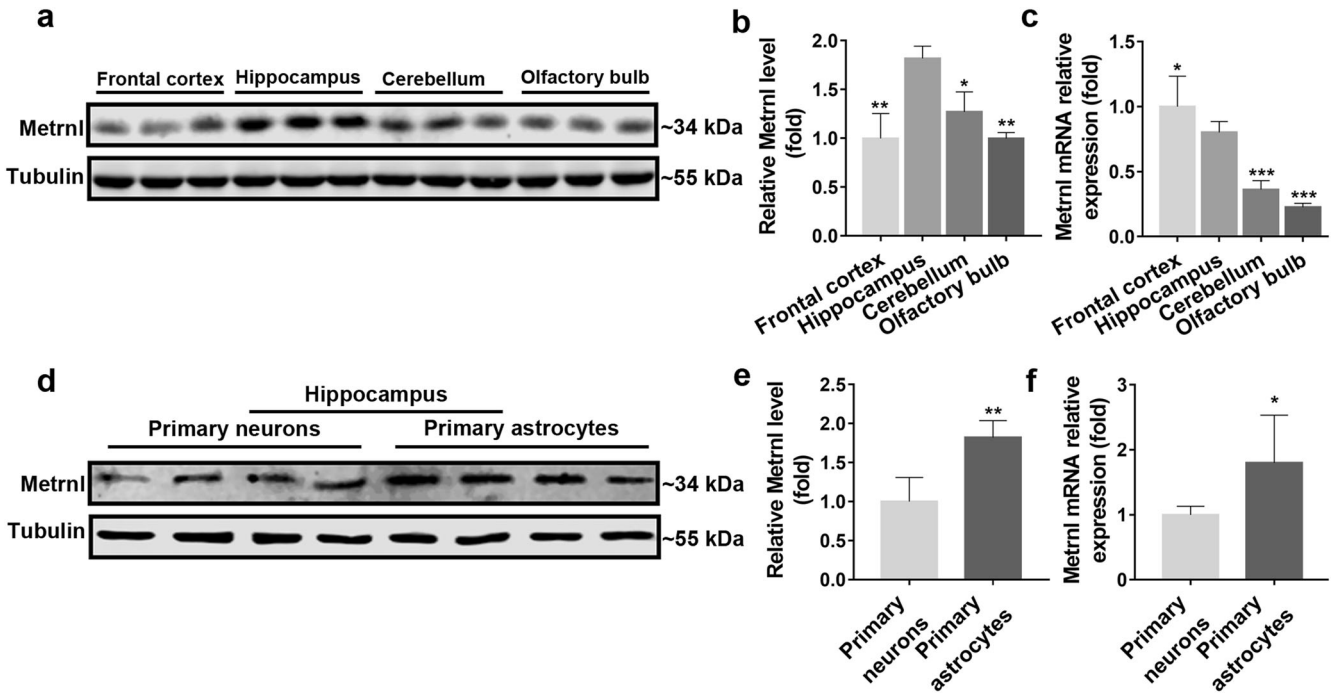


**Fig. 1 Distribution of Metrnl in the central nervous system. a**, **b** Representative Western blots (**a**) and quantitative analysis (**b**) of Metrnl protein expression in different brain regions. $n = 3$ per group, $^{*}P < 0.05$, $^{**}P < 0.01$ versus hippocampus. **c** Metrnl mRNA expression in different brain regions. $n = 6$ per group, $^{*}P < 0.05$, $^{***}P < 0.001$ versus hippocampus. **d**, **e** Representative Western blots (**d**) and quantitative analysis (**e**) of Metrnl protein expression in the hippocampal neurons and astrocytes. $n = 4$ per group, $^{**}P < 0.01$ versus Primary neurons. **f** Metrnl mRNA expression in the hippocampal neurons and astrocytes. $n = 4$ per group, $^{*}P < 0.05$ versus primary neurons. Data are shown as mean ± SD.

anti-mouse antibody (LI-COR IRDye 800CW 926–32212), and the Donkey anti-rabbit antibody (LI-COR IRDye 800CW 926–32213).

### Detection of Metrnl and BDNF levels in the cell supernatant

The Metrnl and BDNF levels in the cell supernatant were detected using ELISA kits (R&D Systems; Minneapolis, MN, USA).

### Detection of oxidative stress indicators

The oxidative stress indicators included Caspase-3, maleic dialdehyde (MDA), glutathione peroxidase (GSH-px) and superoxide dismutase (SOD). These were detected using the respective detection kits (Beyotime Biotechnology; China).

### Statistical analysis

All data are presented as the mean ± SD. Two-way repeated measures ANOVA was performed, followed by Fisher's least significant difference post hoc analysis to assess the escape latency, total swimming distance, and swimming speed, with genotype or treatment as the between-group variation and training days as the within-group variation. The Mann–Whitney *U* test and the Kruskal–Wallis test were performed to compare the frequency of crossing the platform between two groups and among multiple groups, respectively. The Two-tailed Student's *t*-test was performed to compare two groups. A one-way ANOVA was performed, followed by the Fisher's least significant difference post hoc analysis to compare multiple groups. All statistical tests were performed using the SPSS 11.0 software (SPSS Inc.; Chicago, IL, USA). All differences among and between groups were considered to be statistically significant at $P < 0.05$.

## RESULTS

### Distribution of Metrnl in the CNS

Metrnl is a neurotrophic factor whose distribution in the CNS is not clear. We compared the mRNA and protein levels of Metrnl in the frontal cortex, hippocampus, cerebellum, and olfactory bulb. The results showed that the expression of Metrnl was highest in the hippocampus at the protein level, but the Metrnl mRNA level was highest in the frontal cortex and was slightly higher than that in the hippocampus (Fig. 1a–c). We also compared the expression of Metrnl in the hippocampal neurons and astrocytes in vitro and found that the expression of Metrnl was considerably higher in the hippocampal astrocytes than in the hippocampal neurons at both protein and mRNA levels (Fig. 1d–f).

### Metrnl knockout mice in the baseline state displayed no significant changes in learning and memory functions

Metrnl knockout mice were generated by the excision of exon 3 and the coding region of exon 4 of the Metrnl gene, and were verified by genotyping (Fig. 2a, b). The knockout efficiency of Metrnl in the Metrnl knockout mice was verified by performing real-time PCR and ELISA; the results showed that the Metrnl knockout mice did not express Metrnl (Fig. 2c, d). We further compared the learning and memory functions of Metrnl knockout and wild-type control mice by conducting the Morris water maze test. The results showed no significant differences in escape latency, total distance and swimming speed between different genotypes (Fig. 2e, f, i, j). The frequency of crossing the platform and the percentage of time spent in the target quadrant in the probe trial on day 6 also failed to differ significantly between Metrnl knockout and wild-type control mice (Fig. 2g, h, j). These results indicated that in the baseline state, the deficiency in Metrnl did not affect learning and memory functions. We also compared the expression of cognition-related proteins, including BDNF, TrkB, synaptophysin and postsynaptic density protein 95 (PSD95), and found no significant differences in the frontal cortex (Fig. 2k, l) and hippocampus (Fig. 2m, n) between the two groups.

### Metrnl knockout aggravated learning dysfunction in the D-gal-induced aging mice

We established the D-gal-induced aging mouse model and further compared the learning and memory functions of Metrnl knockout

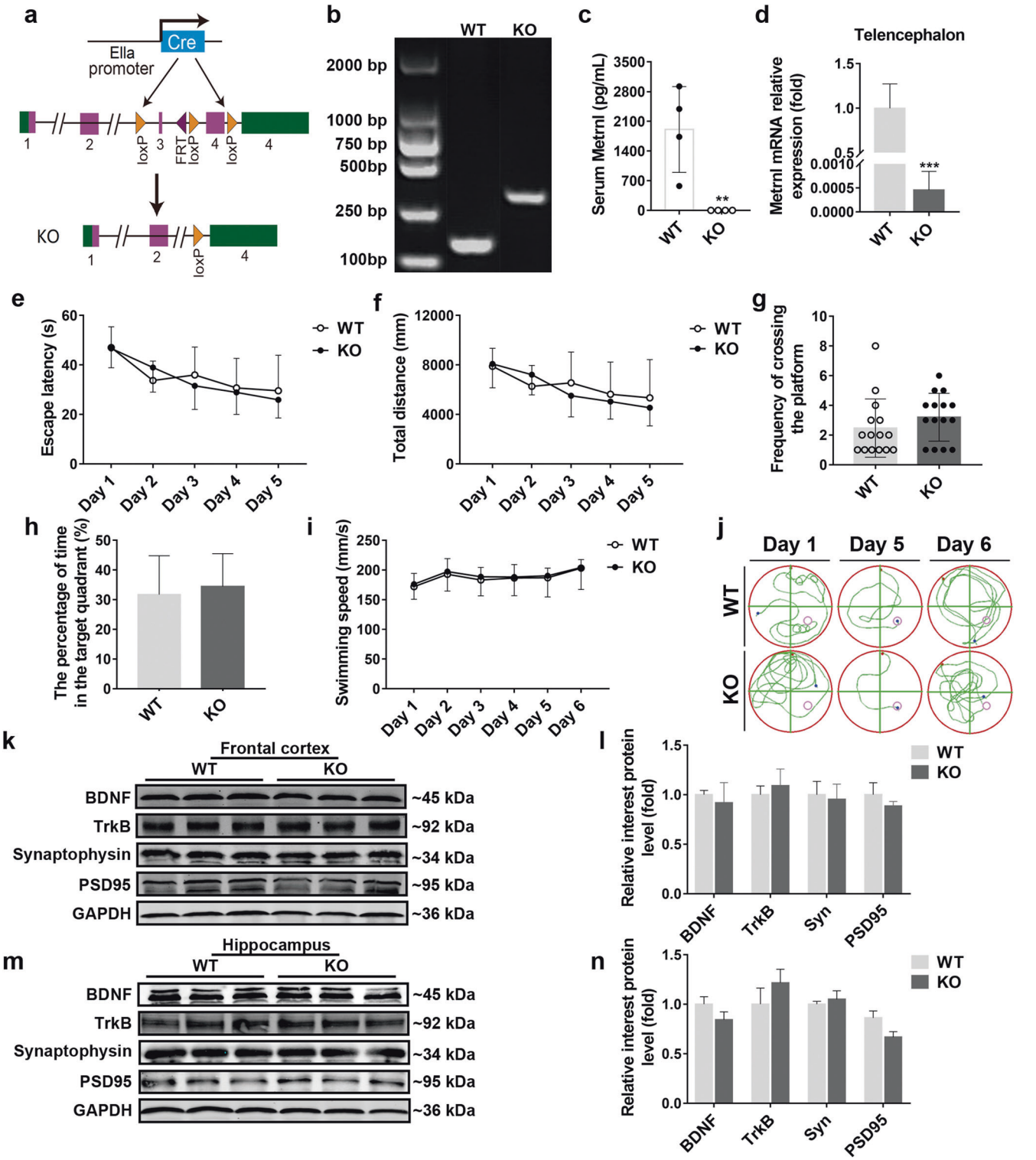


**Fig. 2 Learning and memory functions and cognition-related proteins in the Metrnl knockout mice (KO) and wild-type control mice (WT) in the baseline state. a** Strategy for generating Metrnl KO mice. **b** Genotyping of Metrnl KO and WT mice. **c** Serum Metrnl levels of Metrnl KO and WT mice. $n = 4$ per group, $^{**}P < 0.01$ versus WT. **d** Metrnl mRNA levels in the telencephalon. $n = 4$ per group, $^{***}P < 0.001$ versus WT. **e** Escape latency in the spatial acquisition training during day 1–5 (Group: $F_{(1,28)} = 0.279$, $P > 0.05$; Training days: $F_{(4,112)} = 18.41$, $P < 0.05$). $n = 15$ per group. **f** Total distance in the spatial acquisition training during days 1–5 (Group: $F_{(1,28)} = 0.65$, $P > 0.05$; Training days: $F_{(4,112)} = 10.58$, $P < 0.05$). $n = 15$ per group. **g** Frequency of crossing the platform in the probe trial on day 6. $n = 15$ per group. **h** Percentage of time in the target quadrant in the probe trial on day 6. $n = 15$ per group. **i** Swimming speed during days 1–6 (Group: $F_{(1,28)} = 0.17$, $P > 0.05$; Training days: $F_{(5,140)} = 9.08$, $P < 0.05$). $n = 15$ per group. **j** Representative traces of mice movement on day 1, day 5 and day 6. **k–n** Representative Western blots and quantitative analysis of BDNF, TrkB, synaptophysin and PSD95 protein expression in the frontal cortex (**k**, **l**) and hippocampus (**m**, **n**). $n = 3$ per group. Data are shown as mean ± SD.

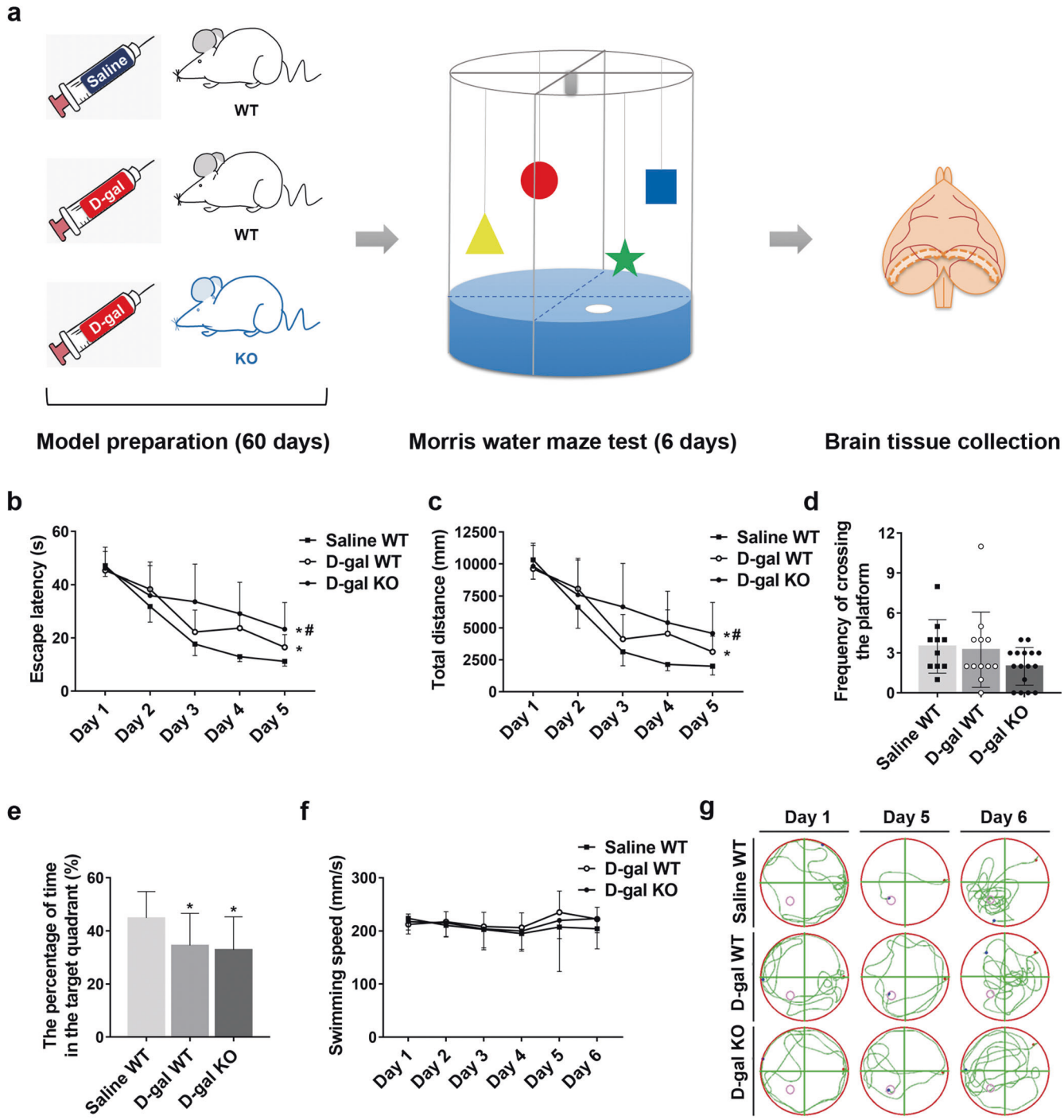


**Fig. 3 Assessment of learning and memory functions in the Metrnl knockout mice (KO) and wild-type control mice (WT) in the D-gal-induced aging model. a** Design of the experiment. Metrnl WT and KO mice were divided into three groups: saline WT group, D-gal WT group and D-gal KO group. D-gal groups were intraperitoneally injected with D-gal (100 mg/kg) for 60 days and saline group was injected with a corresponding volume of saline. The Morris water maze test was conducted to assess the learning and memory functions. After that, the brain tissues of mice were harvested for the next study. **b** Escape latency in spatial acquisition training during days 1–5 (Group: $F_{(2,35)} = 13.02$, $^{*}P < 0.05$ versus Saline WT, $^{\#}P < 0.05$ versus D-gal WT; Training days: $F_{(4,140)} = 95.44$, $P < 0.05$). **c** Total distance in spatial acquisition training during days 1–5 (Group: $F_{(2,35)} = 33.84$, $^{*}P < 0.05$ versus Saline WT, $^{\#}P < 0.05$ versus D-gal WT; Training days: $F_{(4,140)} = 98.28$, $P < 0.05$). **d** Frequency of crossing the platform in probe trial on day 6. **e** The percentage of time in the target quadrant in probe trial on day 6, $^{*}P < 0.05$ versus Saline WT. **f** Swimming speed during day 1–6 (Group: $F_{(2,35)} = 0.15$, $P > 0.05$; Training days: $F_{(5,175)} = 3.47$, $P < 0.05$). **g** Representative traces of mice movement on day 1, day 5 and day 6. $n = 10$ for each saline WT group; $n = 12$ for each D-gal WT group; $n = 16$ for each D-gal KO group. Data are shown as mean ± SD.

and wild-type control mice by conducting the Morris water maze test (see Fig. 3a for the experimental protocol). Overall, all mice showed a decrease in their escape latency and total distance during training (Fig. 3b, c, g). The groups differed significantly in their escape latency, and the total distance (Fig. 3b, c, g). The D-gal-treated mice showed a significantly longer escape latency and traveled a significantly greater total distance than the saline-treated mice. Metrnl deficiency further increased the escape

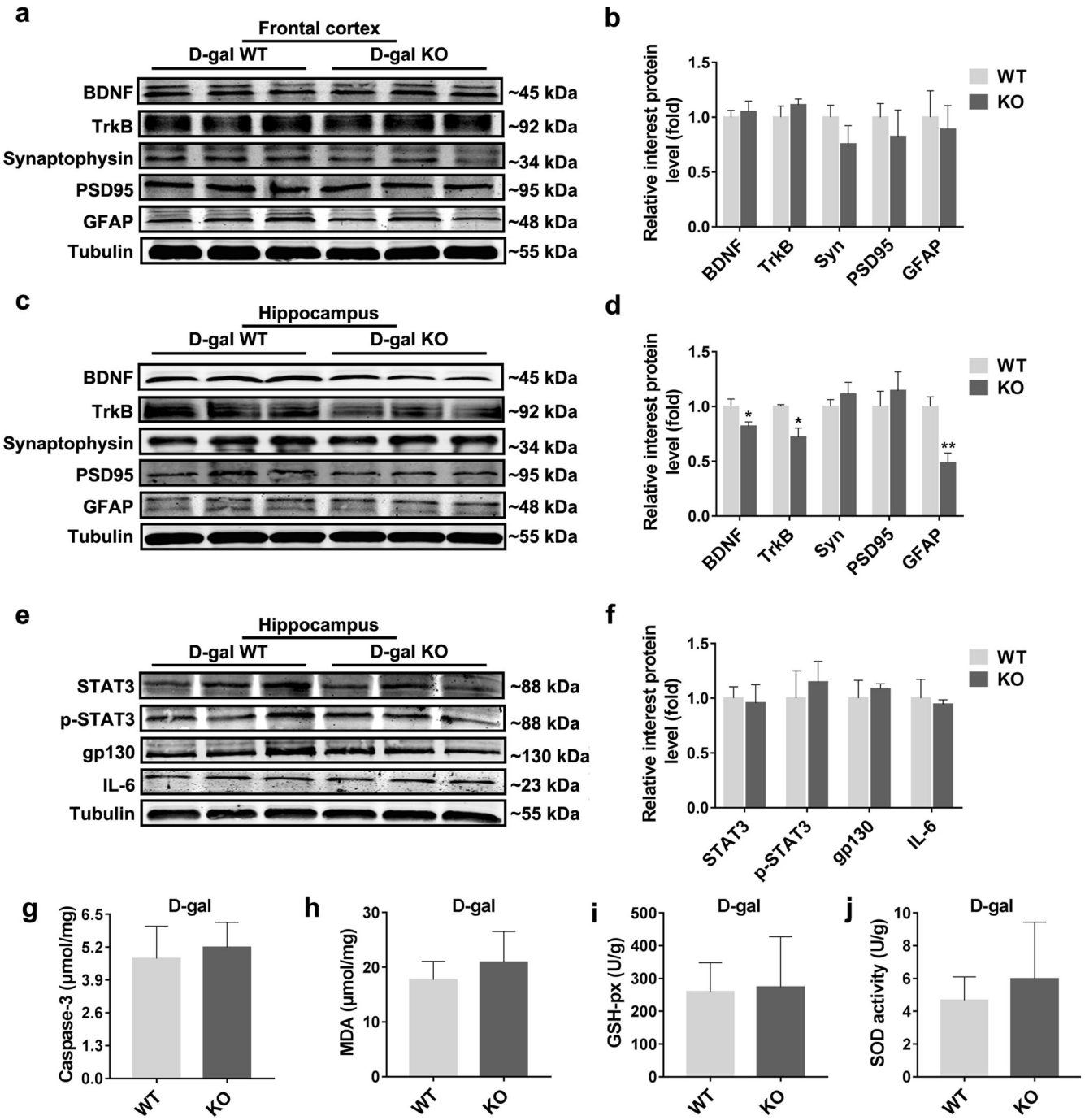


**Fig. 4 Cognition-related proteins, JAK-STAT3 pathway proteins, and oxidative stress indicators of Metrnl knockout mice (KO) and wild-type control mice (WT) in the D-gal-induced aging model. a–d** Representative Western blots and quantitative analysis of BDNF, TrkB, synaptophysin, PSD95 and GFAP protein expression in the frontal cortex (**a**, **b**) and hippocampus (**c**, **d**). $n = 3$ per group, $^{*}P < 0.05$, $^{**}P < 0.01$ versus WT. **e**, **f** Representative Western blots (**e**) and quantitative analysis (**f**) of JAK-STAT3 pathway proteins including STAT3, p-STAT3, gp130, and IL-6 in the hippocampus. $n = 3$ per group**. g–j** Caspase-3 (**g**), MDA (**h**), GSH-px (**i**), and SOD (**j**) levels in the telencephalon. $n = 3$ per group. Data are shown as mean ± SD.

latency and the total distance traveled by the D-gal-treated mice (Fig. 3b, c, g). In the probe trial, the percentage of time spent in the target quadrant by the saline-treated mice was significantly higher than that by the D-gal-treated mice (Fig. 3e, g), but there were no differences between D-gal-treated Metrnl knockout and wild-type mice (Fig. 3e, g). Additionally, all three groups showed a comparable frequency of crossing the platform and swimming speed (Fig. 3d, f, g). These results suggested that D-gal impaired learning and memory functions, and Metrnl deletion further aggravated learning dysfunction.

### Metrnl knockout decreased the hippocampal BDNF levels in the D-gal-induced aging mice

We further studied the effects of Metrnl deficiency on cognition-related proteins in D-gal-induced aging mice. Metrnl knockout decreased the levels of BDNF, TrkB, and GFAP in the hippocampus, but not in the frontal cortex (Fig. 4a–d). We also investigated the JAK-STAT3 pathway which is involved in the regulation of neurite outgrowth by Metrnl [15], but found no differences in the hippocampal STAT3, p-STAT3, IL-6, and the co-receptor gp130 (CD130) levels between the two genotypes in the D-gal induced

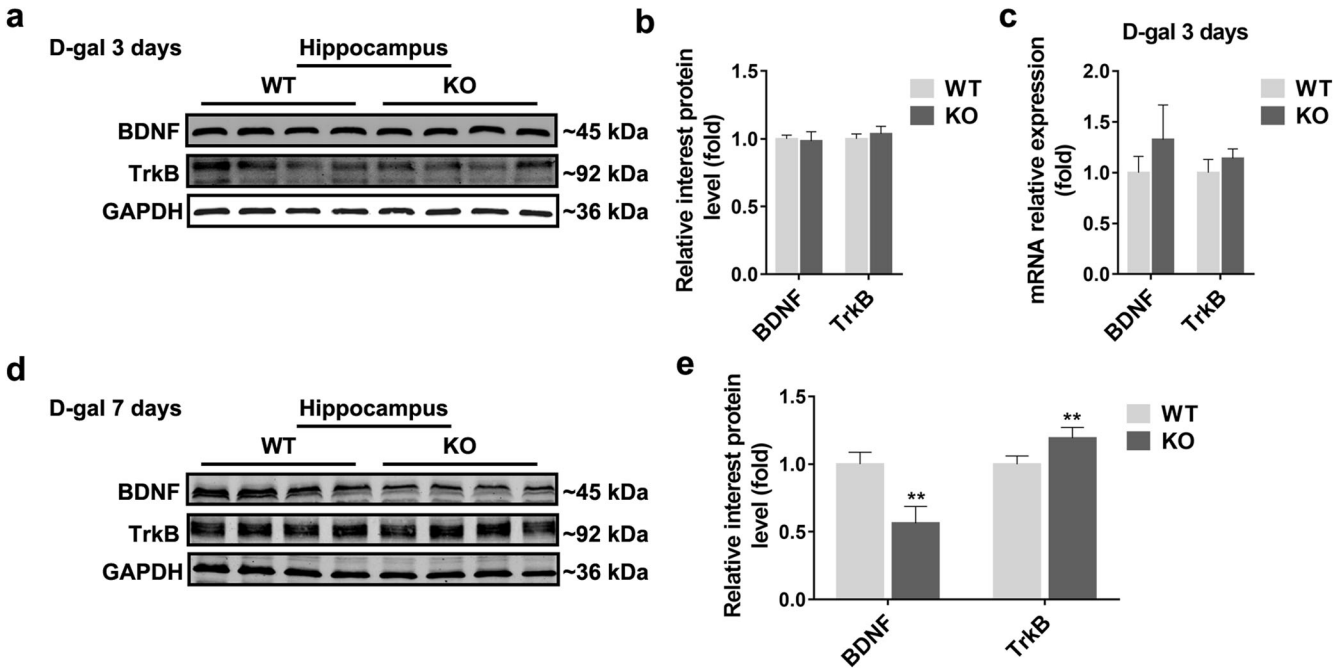


**Fig. 5 Hippocampal BDNF and TrkB levels in the Metrnl knockout mice (KO) and wild-type control mice (WT) after intraperitoneal injection of D-gal for three and seven days. a, b** Representative Western blots (**a**) and quantitative analysis (**b**) of hippocampal BDNF and TrkB protein expression after intraperitoneal injection of D-gal for three days. $n = 4$ per group. **c** BDNF and TrkB mRNA expression in the hippocampus after intraperitoneal injection of D-gal for three days. $n = 4$ per group. **d**, **e** Representative Western blots (**d**) and quantitative analysis (**e**) of hippocampal BDNF and TrkB protein expression after intraperitoneal injection of D-gal for seven days. $n = 4$ per group, $^{**}P < 0.01$ versus WT. Data are shown as mean ± SD.

aging model (Fig. 4e, f). Our results (Supplementary Fig. 1c–f) and those reported in previous studies indicated that oxidative stress and apoptosis were the major causes of cognitive impairment in the D-gal-induced aging model [17]. We further tested oxidative stress and apoptosis in the Metrnl knockout and wild-type mice after treatment with D-gal, but found no significant changes in the levels of the Caspase-3, MDA, GSH-px, and SOD between the two genotypes (Fig. 4g–j).

### Metrnl knockout reduced hippocampal BDNF levels in the early stage of the D-gal-induced aging mouse model

To determine the time course for the reduction of hippocampal BDNF levels caused by Metrnl knockout, we determined the hippocampal BDNF levels in the Metrnl knockout and wild-type mice after intraperitoneal administration of D-gal for three and seven days. No significant differences were found in the hippocampal BDNF and TrkB levels between Metrnl knockout and wild-type mice after administration of D-gal for three days (Fig. 5a–c). However, after administration of D-gal for seven days, Metrnl knockout significantly decreased BDNF levels, and increased TrkB levels in the hippocampus (Fig. 5d, e). These results indicated that Metrnl knockout might reduce hippocampal BDNF levels in the early stage of the D-gal-induced aging model.

### Metrnl did not affect the BDNF levels in the primary hippocampal neurons of the D-gal-induced aging model in vitro

Hippocampal Metrnl increased in the D-gal-induced aging mice in vivo (Supplementary Fig. 1g–i). Thus, we determined the Metrnl levels in the primary hippocampal neurons of the D-gal model in vitro but found no significant changes (Fig. 6a–c). To further investigate the effect of Metrnl on hippocampal neurons, lentivirus-mediated Metrnl knockdown and overexpression were conducted in the primary hippocampal neurons (Fig. 6d, g). The Metrnl knockdown or overexpression did not significantly change the expression of BDNF and TrkB in the hippocampal neurons of the D-gal model in vitro (Fig. 6e, f, h, i).

### Metrnl regulated the BDNF levels in the primary hippocampal astrocytes of the D-gal-induced aging model in vitro

We also determined the changes in Metrnl in the primary hippocampal astrocytes of the D-gal model in vitro and found that the mRNA and protein levels of Metrnl in the hippocampal astrocytes increased significantly (Fig. 7a–c). Lentivirus-mediated knockdown and overexpression of Metrnl were conducted in the primary hippocampal astrocytes to further determine the effect of Metrnl on hippocampal astrocytes (Fig. 7d, i). In the D-gal model of hippocampal astrocytes in vitro, Metrnl knockdown reduced the BDNF levels (Fig. 7d, e, g, h), while Metrnl overexpression increased the expression and secretion of BDNF (Fig. 7i–m).

## DISCUSSION

In this study, we showed that Metrnl deficiency aggravates cognitive dysfunction and downregulates the hippocampal BDNF levels during the aging process. Our main findings were as follows: (a) Metrnl protein levels were higher in the hippocampus than in the other three brain regions, and the mRNA and protein levels of Metrnl in the hippocampal astrocytes were considerably higher in the hippocampal astrocytes than in the hippocampal neurons in vitro. (b) Metrnl deficiency did not influence the learning and memory functions of mice or the BDNF levels in the baseline state. However, in the D-gal-induced aging mouse model, Metrnl knockout aggravated the aging-related learning impairment in mice and downregulated their hippocampal BDNF levels. (c) Metrnl knockout reduced hippocampal BDNF levels in the early stage of the D-gal-induced aging mouse model. (d) In the D-gal model of hippocampal astrocytes in vitro, Metrnl overexpression increased the BDNF levels, and Metrnl knockdown decreased the BDNF levels.

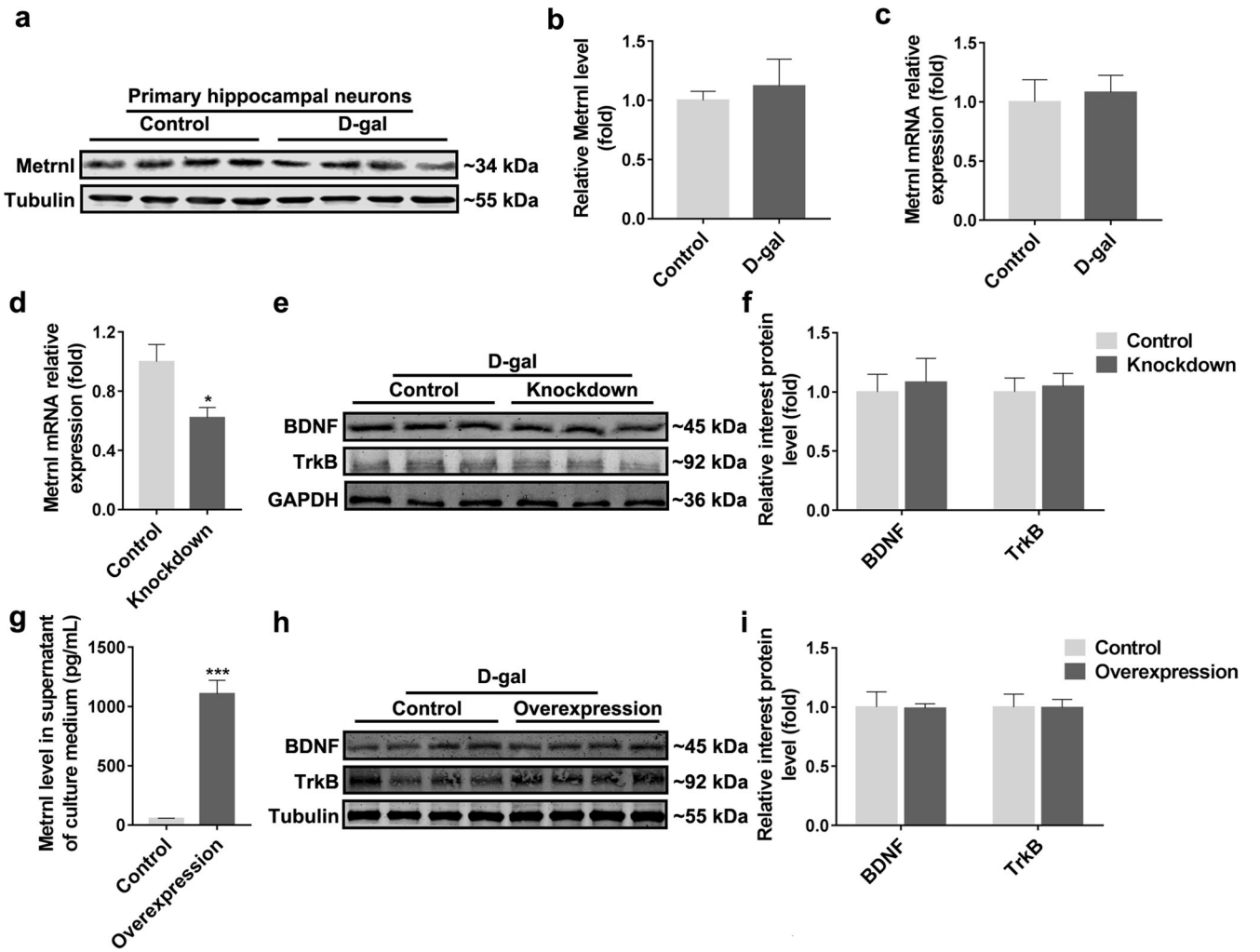


**Fig. 6 Effects of Metrnl knockdown and overexpression on BDNF and TrkB levels in the D-gal model of primary hippocampal neurons in vitro. a**, **b** Representative Western blots (**a**) and quantitative analysis (**b**) of Metrnl protein expression in the neurons. $n = 4$ per group. **c** Metrnl mRNA expression in neurons. $n = 4$ per group. **d** Knockdown of Metrnl by lentivirus transfection in the neurons. $n = 5$ per group, $^{*}P < 0.05$ versus Control. **e**, **f** Representative Western blots (**e**) and quantitative analysis (**f**) of BDNF and TrkB protein expression in the neurons after Metrnl knockdown. $n = 3$ per group. **g** Concentration of Metrnl in the supernatant of neurons after Metrnl overexpression. $n = 5$ per group, $^{***}P < 0.001$ versus Control. **h, i** Representative Western blots (**h**) and quantitative analysis (**i**) of BDNF and TrkB protein expression in the neurons after Metrnl overexpression. $n = 4$ per group. Data are shown as mean ± SD.

Aging impairs learning and memory functions and increases the risk of dementia [24]. The D-gal-induced aging model is widely used for studying aging and aging-related cognitive impairment [17]. Chronic administration of D-gal not only causes mitochondrial dysfunction but also increases oxidative stress, inflammation, and apoptosis, decreases BDNF levels, and finally, leads to cognitive dysfunction [16]. In this study, we successfully prepared the D-gal-induced aging mouse model and reproduced the typical features of this model, including learning and memory dysfunctions and low expression of BDNF (Fig. 3 and Supplementary Fig. 1). The hippocampal Metrnl levels in the D-gal-induced aging mice increased significantly (Supplementary Fig. 1g–i), suggesting that Metrnl might be related to aging-related cognitive dysfunction. The Morris water maze test is a primary method to assess learning and memory and is probably the most widely used behavioral test for studying cognitive functions in rodents [25, 26]. Hence, we investigated the effects of Metrnl on the cognitive functions in the D-gal-induced aging model by conducting the Morris water maze test and found that Metrnl knockout aggravated aging-related learning dysfunction (Fig. 3). These results indicated that Metrnl regulates learning function during the aging process and has a protective effect on aging-related learning impairment. In the D-gal-induced aging mouse model, Metrnl knockout aggravates learning deficit but does not significantly reduce memory function, although there is a reduction trend. Thus, Metrnl mainly regulates learning rather than memory; however, further studies need to be performed to verify this.

BDNF is an important member of the neurotrophin family mainly and is secreted by neurons and astrocytes. It promotes the survival and differentiation of neural cells, participates in axonal growth, modulates synaptic plasticity, and strongly affects cognitive functions [27]. Moreover, BDNF is the most abundant protein among the neurotrophin family members, especially in the hippocampus, which is closely associated with learning and memory functions [28, 29]. In the D-gal-induced aging mouse model, a decrease in the level of BDNF is a primary reason for aging-related cognitive impairment [16]. In this study, we found that Metrnl knockout aggravated the decrease in hippocampal BDNF levels in the D-gal induced aging mice. These findings were consistent with the poorer learning function of Metrnl knockout mice than of the wild-type mice in the D-gal-induced aging

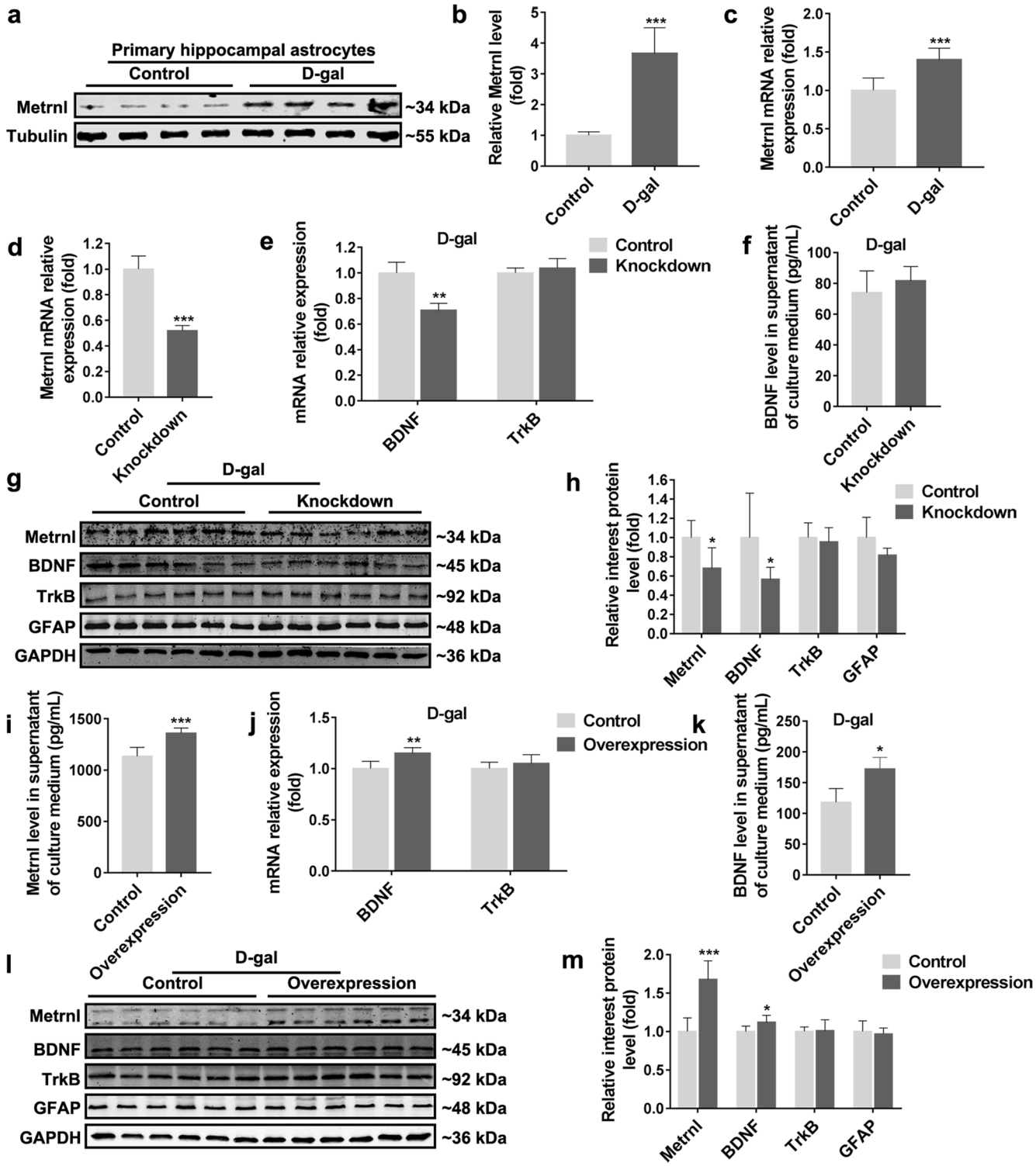


**Fig. 7 Effects of Metrnl knockdown and overexpression on BDNF and TrkB levels in the D-gal model of primary hippocampal astrocytes in vitro. a**, **b** Representative Western blots (**a**) and quantitative analysis (**b**) of Metrnl protein expression in the astrocytes. $n = 4$ per group, $^{***}P < 0.001$ versus Control. **c** Metrnl mRNA expression in the astrocytes. $n = 4$ per group, $^{***}P < 0.001$ versus Control. **d** Knockdown of Metrnl by lentivirus transfection in the astrocytes. $n = 6$ per group, $^{***}P < 0.001$ versus Control. **e** BDNF and TrkB mRNA expression in the astrocytes after Metrnl knockdown. $n = 5$ per group, $^{**}P < 0.01$ versus Control. **f** Concentration of BDNF in the supernatant of astrocytes after Metrnl knockdown. $n = 6$ per group. **g**, **h** Representative Western blots (**g**) and quantitative analysis (**h**) of Metrnl, BDNF, TrkB, and GFAP protein expression in the astrocytes after Metrnl knockdown. $n = 6$ per group, $^{*}P < 0.05$ versus Control. **i** Concentration of Metrnl in the supernatant of astrocytes after Metrnl overexpression by lentivirus transfection. $n = 6$ per group, $^{***}P < 0.001$ versus Control. **j** BDNF and TrkB mRNA levels in the astrocytes after Metrnl overexpression. $n = 6$ per group, $^{**}P < 0.01$ versus Control. **k** Concentration of BDNF in the supernatant of astrocytes after Metrnl overexpression. $n = 4$ per group, $^{*}P < 0.05$ versus Control. **l**, **m** Representative Western blots (**l**) and quantitative analysis (**m**) of Metrnl, BDNF, TrkB, and GFAP protein expression in the astrocytes after Metrnl overexpression. $n = 6$ per group, $^{*}P < 0.05$, $^{***}P < 0.001$ versus Control. Data are shown as mean ± SD.

condition (Figs. 3b, c, g; 4c, d). TrkB is the specific receptor for BDNF in the CNS and is necessary for cognitive functions [30, 31]. Therefore, we also evaluated the TrkB levels to determine whether the changes in the TrkB levels were similar to those of the BDNF levels. Overall, changes in the TrkB levels were not consistent with the changes in BDNF and Metrnl levels, which indicated that Metrnl does not directly affect TrkB. However, as the specific receptor of BDNF, TrkB levels can be influenced by BDNF to a certain extent [31]. The changes in BDNF levels caused by Metrnl might partly affect TrkB levels, but the effect might not be significant since TrkB acts as a receptor not only for BDNF but also for other neurotrophic factors. Thus, changes in other neurotrophic factors during aging can also affect TrkB levels. The effect of Metrnl on learning function is more closely related to hippocampal BDNF than TrkB, but whether Metrnl regulates the learning function via hippocampal BDNF still needs to be verified.

Astrocytes have important physiological functions and affect synaptic activity and plasticity, neuronal network oscillations, and cognitive functions [32]. In the pathological brain condition, astrocyte impairment can lead to cognitive dysfunction [33]. In patients with aging-related Alzheimer's disease, the changes in the astrocyte skeleton structure occur even before amyloid deposition and have a significant effect on cognitive functions [34, 35]. We found that the GFAP (a specific biological marker of astrocyte) levels in the Metrnl knockout mice were lower than those in the Metrnl wild-type mice in the frontal cortex and hippocampus (data not shown), although the Metrnl knockout mice did not show learning and memory impairment in the baseline state. Moreover, in the D-gal-induced aging mouse model, Metrnl deficiency aggravated the reduction in the GFAP levels in the hippocampus (Fig. 4c, d), which was similar to the changes in the BDNF levels. Additionally, the expression of Metrnl in the hippocampal astrocytes was higher than that in the in neurons (Fig. 1d–f). These results suggested that there might be associations among Metrnl, hippocampal BDNF, and hippocampal astrocytes, and Metrnl might regulate the hippocampal BDNF levels via hippocampal astrocytes.

To verify the above speculation, we developed the D-gal-induced aging cell model and evaluated the changes of Metrnl levels in the hippocampal astrocytes and neurons. We found that the Metrnl levels were significantly increased in the D-gal-induced aging cell model of hippocampal astrocytes but not neurons (Figs. 6a–c; 7a–c). We further investigated the effects of Metrnl on BDNF in the D-gal model of neurons and astrocytes in vitro and found that Metrnl can regulate the BDNF levels in the hippocampal astrocytes but not neurons (Figs. 6; 7). In the D-gal-induced aging cell model in vitro, Metrnl knockdown reduced the mRNA and protein levels of BDNF in hippocampal astrocytes (Fig. 7e, g, h), and Metrnl overexpression increased the BDNF levels (Fig. 7j–m). These results further indicated that Metrnl could regulate the BDNF levels in hippocampal astrocytes during the aging process.

However, in the D-gal-induced aging cell model in vitro, Metrnl knockdown did not significantly reduce the GFAP levels in the hippocampal astrocytes (Fig. 7g, h), which differed from the finding that Metrnl knockout significantly reduced GFAP levels in vivo. GFAP is not only the main intermediate filament protein in astrocytes but is also an important component of the cytoskeleton in astrocytes. It helps to maintain the mechanical strength and shape of the cells [36]. GFAP degrades slowly (like other intermediate filament proteins) with a degradation half-life of approximately a month [37]. In Metrnl knockout mice, the Ella-Cre-induced deletion of Metrnl in mice occurs at the embryonic stage, which gives Metrnl enough time to affect the expression of GFAP in vivo. However, the duration of Metrnl overexpression or knockdown in the astrocytes in vitro is considerably shorter than the half-life of GFAP. The time available for Metrnl to change the GFAP levels in vitro is insufficient, even if it does work. This might be the main reason for the inconsistent results of GFAP in vivo and in vitro.

Aging is the main risk factor for cognitive impairment and neurodegenerative diseases [38]. During the aging process, a decrease in the BDNF levels and abnormalities in astrocyte function lead to cognitive impairment [39]. We found that Metrnl affected the learning function, hippocampal BDNF and GFAP levels during the aging process, suggesting that Metrnl, hippocampal BDNF, astrocytes, and the learning function might be associated. Metrnl might regulate hippocampal BDNF levels through hippocampal astrocytes and improve aging-related learning impairment. However, further studies need to be conducted to obtain more direct evidence. In follow-up studies, astrocyte-specific Metrnl knockout mice need to be developed to verify the above mentioned speculation.

To summarize, in this study, we found that Metrnl regulates cognitive functions and hippocampal BDNF levels during the aging process and affects hippocampal BDNF levels in the early stage. As a novel neurotrophic factor and an endogenous protein, Metrnl might be a new target for treating aging-related cognitive impairment.

## ACKNOWLEDGEMENTS

This work was supported by grants from the National Natural Science Foundation of China (№82104166, №81730098 and №82030110), Medical Innovation Major Project (№16CXZ009), and Shanghai Science and Technology Commission Project (№21140901000).

## AUTHOR CONTRIBUTIONS

CH and ZW performed most of the experiments and data analyses and wrote the paper. SLZ, WJH, SNW and YZ performed some experiments and/or data analysis. CYM designed the study, performed data analysis, and wrote and revised the paper.

## ADDITIONAL INFORMATION

**Supplementary information** The online version contains supplementary material available at https://doi.org/10.1038/s41401-022-01009-y.

**Competing interests:** The authors declare no competing interests.

## REFERENCES

1. James GA, Kearney-Ramos TE, Young JA, Kilts CD, Gess JL, Fausett JS. Functional independence in resting-state connectivity facilitates higher-order cognition. Brain Cogn. 2016;105:78–87.
2. 2021 Alzheimer's disease facts and figures. Alzheimers Dement. 2021;17:327–406.
3. Janota C, Lemere CA, Brito MA. Dissecting the contribution of vascular alterations and aging to Alzheimer's disease. Mol Neurobiol. 2016;53:3793–811.
4. Jia L, Quan M, Fu Y, Zhao T, Li Y, Wei C, et al. Dementia in China: epidemiology, clinical management, and research advances. Lancet Neurol. 2020;19:81–92.
5. Sahakian BJ, Bruhl AB, Cook J, Killikelly C, Savulich G, Piercy T, et al. The impact of neuroscience on society: cognitive enhancement in neuropsychiatric disorders and in healthy people. Philos Trans R Soc Lond B Biol Sci. 2015. https://doi.org/10.1098/rstb.2014.0214.
6. Haapasalo A, Hiltunen M. A report from the 8th Kuopio Alzheimer Symposium. Neurodegener Dis Manag. 2018;8:289–99.
7. Li ZY, Zheng SL, Wang P, Xu TY, Guan YF, Zhang YJ, et al. Subfatin is a novel adipokine and unlike Meteorin in adipose and brain expression. CNS Neurosci Ther. 2014;20:344–54.
8. Li ZY, Song J, Zheng SL, Fan MB, Guan YF, Qu Y, et al. Adipocyte metrnl antagonizes insulin resistance through PPAR-γ signaling. Diabetes. 2015;64:4011–22.
9. Li ZY, Fan MB, Zhang SL, Qu Y, Zheng SL, Song J, et al. Intestinal Metrnl released into the gut lumen acts as a local regulator for gut antimicrobial peptides. Acta Pharmacol Sin. 2016;37:1458–66.
10. Zheng SL, Li ZY, Song J, Liu JM, Miao CY. Metrnl: a secreted protein with new emerging functions. Acta Pharmacol Sin. 2016;37:571–9.
11. Qi Q, Hu WJ, Zheng SL, Zhang SL, Le YY, Li ZY, et al. Metrnl deficiency decreases blood HDL cholesterol and increases blood triglyceride. Acta Pharmacol Sin. 2020;41:1568–75.

12. Miao ZW, Hu WJ, Li ZY, Miao CY. Involvement of the secreted protein Metrnl in human diseases. Acta Pharmacol Sin. 2020;41:1525–30.
13. Zhang SL, Li ZY, Wang DS, Xu TY, Fan MB, Cheng MH, et al. Aggravated ulcerative colitis caused by intestinal Metrnl deficiency is associated with reduced autophagy in epithelial cells. Acta Pharmacol Sin. 2020;41:763–70.
14. Surace C, Piazzolla S, Sirleto P, Digilio MC, Roberti MC, Lombardo A, et al. Mild ring 17 syndrome shares common phenotypic features irrespective of the chromosomal breakpoints location. Clin Genet. 2009;76:256–62.
15. Jorgensen JR, Fransson A, Fjord-Larsen L, Thompson LH, Houchins JP, Andrade N, et al. Cometin is a novel neurotrophic factor that promotes neurite outgrowth and neuroblast migration in vitro and supports survival of spiral ganglion neurons in vivo. Exp Neurol. 2012;233:172–81.
16. Shwe T, Pratchayasakul W, Chattipakorn N, Chattipakorn SC. Role of D-galactose-induced brain aging and its potential used for therapeutic interventions. Exp Gerontol. 2018;101:13–36.
17. Ali T, Badshah H, Kim TH, Kim MO. Melatonin attenuates D-galactose-induced memory impairment, neuroinflammation and neurodegeneration via RAGE/NF-K B/JNK signaling pathway in aging mouse model. J Pineal Res. 2015;58:71–85.
18. Azman KF, Zakaria R. D-Galactose-induced accelerated aging model: an overview. Biogerontology. 2019;20:763–82.
19. Dooley TP, Miranda M, Jones NC, Depamphilis ML. Transactivation of the adenovirus EIIa promoter in the absence of adenovirus E1A protein is restricted to mouse oocytes and preimplantation embryos. Development. 1989;107:945–56.
20. Vorhees CV, Williams MT. Morris water maze: procedures for assessing spatial and related forms of learning and memory. Nat Protoc. 2006;1:848–58.
21. Wang SN, Xu TY, Wang X, Guan YF, Zhang SL, Wang P, et al. Neuroprotective efficacy of an aminopropyl carbazole derivative P7C3-A20 in ischemic stroke. CNS Neurosci Ther. 2016;22:782–8.
22. Prah J, Winters A, Chaudhari K, Hersh J, Liu R, Yang SH. A novel serum free primary astrocyte culture method that mimic quiescent astrocyte phenotype. J Neurosci Methods. 2019;320:50–63.
23. Chen L, Yao H, Chen X, Wang Z, Xiang Y, Xia J, et al. Ginsenoside Rg1 decreases oxidative stress and down-regulates Akt/mTOR signalling to attenuate cognitive impairment in mice and senescence of neural stem cells induced by D-galactose. Neurochem Res. 2018;43:430–40.
24. Navarro Negredo P, Yeo RW, Brunet A. Aging and rejuvenation of neural stem cells and their niches. Cell Stem Cell. 2020;27:202–23.
25. Weitzner DS, Engler-Chiurazzi EB, Kotilinek LA, Ashe KH, Reed MN. Morris Water Maze Test: optimization for mouse strain and testing environment. J Vis Exp. 2015. https://doi.org/10.3791/52706.
26. Tucker LB, Velosky AG, Mccabe JT. Applications of the Morris water maze in translational traumatic brain injury research. Neurosci Biobehav Rev. 2018;88:187–200.
27. Kumar A, Pareek V, Faiq MA, Kumar P, Raza K, Prasoon P, et al. Regulatory role of NGFs in neurocognitive functions. Rev Neurosci. 2017;28:649–73.
28. Paul J, Gottmann K, Lessmann V. NT-3 regulates BDNF-induced modulation of synaptic transmission in cultured hippocampal neurons. Neuroreport. 2001;12:2635–9.
29. Hofer M, Pagliusi SR, Hohn A, Leibrock J, Barde YA. Regional distribution of brain-derived neurotrophic factor mRNA in the adult mouse brain. EMBO J. 1990;9:2459–64.
30. Eggert S, Kins S, Endres K, Brigadski T. Brothers in arms: proBDNF/BDNF and sAPPα/β-signaling and their common interplay with ADAM10, TrkB, p75NTR, sortilin, and sorLA in the progression of Alzheimer's disease. Biol Chem. 2022;403:43–71.
31. Andreska T, Luningschror P, Sendtner M. Regulation of TrkB cell surface expression-a mechanism for modulation of neuronal responsiveness to brain-derived neurotrophic factor. Cell Tissue Res. 2020;382:5–14.
32. Santello M, Toni N, Volterra A. Astrocyte function from information processing to cognition and cognitive impairment. Nat Neurosci. 2019;22:154–66.
33. Dallerac G, Rouach N. Astrocytes as new targets to improve cognitive functions. Prog Neurobiol. 2016;144:48–67.
34. Yeh CY, Vadhwana B, Verkhratsky A, Rodriguez JJ. Early astrocytic atrophy in the entorhinal cortex of a triple transgenic animal model of Alzheimer's disease. ASN Neuro. 2011;3:271–9.
35. Olabarria M, Noristani HN, Verkhratsky A, Rodriguez JJ. Concomitant astroglial atrophy and astrogliosis in a triple transgenic animal model of Alzheimer's disease. Glia. 2010;58:831–8.
36. van Bodegraven EJ, van Asperen JV, Robe PAJ, Hol EM. Importance of GFAP isoform-specific analyses in astrocytoma. Glia. 2019;67:1417–33.
37. Messing A, Brenner M. GFAP at 50. ASN Neuro. 2020. https://doi.org/10.1177/1759091420949680.
38. Mather M. Aging and cognition. Wiley Interdiscip Rev Cogn Sci. 2010;1:346–62.
39. Chen X, Li Y, Chen W, Nong Z, Huang J, Chen C. Protective effect of hyperbaric oxygen on cognitive impairment induced by D-galactose in mice. Neurochem Res. 2016;41:3032–41.